(Draft)Laser-Based Wireless Communication for Underwater Robots Using a Solar Array Detector

Benjamin Wittrup and Fengying Dang*

***Abstract*—Untethered autonomous underwater vehicles (AUVs) are increasing in popularity in multiple fields. However low-latency, high-speed communication remains an obstacle in their development. Solar arrays present a cost-effective, low-bandwidth detector for an optical communication scheme with eased link alignment requirements. The goal of this study is to develop an optical underwater wireless communication system capable of operating on a low-power underwater robot. To achieve this goal, a pulse-distance modulation scheme, a solar array-based receiver, and associated circuitry were developed. Experiments in water were conducted with both overhead lighting and in a dark room using a commercially available blue-light laser and solar panel. The results show promise for low-cost underwater systems, but indicate that ambient light has a significant impact on solar array-based underwater communication systems.**

***Index Terms*—Marine Robotics, Underwater Wireless Optical Communication, Solar Array, Wireless Communication and Control.**

I. Introduction

Underwater robotics is a developing field with a broad range of applications, including undersea cable maintenance, mineral resource exploration and exploitation, sea floor mapping, and naval mine removal [1]–[3]. In particular, underwater robots are used extensively by the offshore oil and gas industry for exploration, construction and maintenance [1]. Unmanned submersibles are capable of longer, safer, and less costly underwater operations than their manned counterparts, and are classified into two categories: tethered Remotely Operated Vehicles (ROVs), and untethered Autonomous Underwater Vehicles (AUVs). ROV tethers allow for high speed communication and power transmission, enabling real-time control and communication with a human operator and extended operation times [4]. However, tethers limit a vehicle's maneuverability and range while introducing additional costs and the risk of snagging or snapping [5]. As battery technology improves and the cost per energy capacity decreases, untethered AUVs with long operational times are becoming cheaper and more common [6], [7].

While solutions for AUV power availability are being developed, the cost of high-speed wireless communications remains a barrier to AUV development and deployment with real-time control. Historically, underwater communication has been achieved acoustically. These systems are limited to low data rates (kbps) and suffer from high latency and cost, directing much attention to be placed on Underwater Wireless Optical Communication (UWOC) to address these shortcomings [8], [9]. Laser systems capable of high data rates show promise for short to moderate link ranges with high data confidentiality [10], [11]. These systems utilize lasers with emission peaks near the absorption minimum for water in the optical range at 450 nm, with scattering effects resulting in higher wavelengths performing better in more turbid waters [12]. High-sensitivity single-photon detectors, such as avalanche photodiodes (APDs) and positive-instrinsic-negative (PIN) photodiodes, are often used as receivers, trading high sensitivity for smaller active areas and receiving angles [13]–[15]. This tradeoff complicates the problem of link alignment for underwater robotics applications where both the transmitting and receiving craft may be mobile at 6 degrees of freedom [16].

In contrast to APDs and PIN detectors, solar arrays possess limited bandwidth but much larger reception areas, and are widely available in various form factors, making them ideal for low-cost underwater AUVs. In [17], the researchers utilize a solar array with a quadrature amplitude modulation (QAM) orthogonal frequency division multiplexing (OFDM) modulation scheme with a 405 nm laser to transmit over a 7 meter tap water channel under laboratory lighting, achieving data rates as high as 22.56 Mbps using 64-QAM. Additionally, they note that their solar array has a receiving angle of 20°, significantly higher than a lens-less APD- or PIN-based system. Similar modulation schemes with QAM-OFDM have been implemented using high sensitivity detectors, some with even higher data rates [13]–[15]. In [18], [19], Tong *et. al.* develop a series-connected solar array with no-return-to-zero On-Off Keying (NRZ-OOK) modulation to achieve an 18 Mbps maximum data rate over an 80 m underwater channel in laboratory conditions. They utilized a bandpass filter and a baseline compensator to account for the baseline drift arising from the low-frequency cutoff.

While these laser communication schemes have demonstrated data rates far higher than currently available with acoustic communications, the experimental setups have utilized high-power, specialized equipment, usually benchtop arbitrary waveform generators (AWGs) to modulate the laser, digital oscilloscopes to sample and record the received signal at high speeds, and a modern personal computer to demodulate the signal offline. Translating this architecture for real-time AUV controls applications would require a receiving system

B. Wittrup (bowittru@mtu.edu) and F. Dang (fdang1@mtu.edu) are with the Department of Electrical and Computer Engineering, Michigan Technological University, Houghton, MI 49931 USA.

∗Fengying Dang is the corresponding author.

with access to high-speed computing and sampling, capable of digitally demodulating the signal while simultaneously receiving data. Such applications would increase power demand and complexity, limiting the potential of this form of UWOC to be widely used for low-power, low-cost applications. For small, highly-maneuverable, and cost-effective robots, an embedded hardware solution is desirable [20]–[22].

In this paper, we present a novel UWOC scheme operating using off-the-shelf microcontroller, solar array, and laser module hardware for small underwater robotic control, referred to as the Sub-aquatic Hyper-Amplified Real-time Communication System (SHARCS). Our main contributions are: (1) proposing a laser-solar panel communication scheme; (2) implementing pulse-distance modulation (PDM) with custom transmitter and receiver circuits; and (3) conducting extensive experiments under varying ambient lighting conditions to validate this scheme. This approach using commercially available laser and solar panel hardware offers a promising, low-cost solution for short-range wireless communication and control of small to medium-sized underwater robots.

The remainder of the paper is organized as follows. Section II describes the hardware and software for SHARCS. Section III-A discusses the experimental setup under laboratory conditions, and Section III-B discusses the experimental setup for experiments in a realistic environment. Section IV presents the results of the experiments and provides analysis on the performance of SHARCS. Final remarks are provided in Section V.

II. Circuitry and Software

This work considers a one-way, two-party communication network, between a transmitting "main" agent and a receiving "sub" agent. The sub agent possesses the solar panel receiver, and is assumed to have limited energy reserves, thus requiring low-power electronics and not possessing a laser module. The main agent possesses the laser module, and is assumed to possess abundant power and be able to accurately determine the location of the sub agent for purposes of link alignment.

A. Transmitter Circuitry Design

Utilizing low-power, single-core microcontrollers presents a theoretical limit for transmission rate. The overall baud rate of the communications system will be limited not only by the maximum sample rate of the microcontroller, but also its ability to store and process the data as it is received. PDM was selected for this application for its simplicity of demodulation, allowing for processing to occur in between pulses, and because it works well with an active high-pass filter connected to the solar panel. Additionally, PDM can be implemented without requiring high-frequency sampling from an ADC, and can utilize the microcontroller timer modules and interrupt controller, both separate from the CPU, to control pulse detection and decoding. In our scheme, a pulse distance of 400 μs represents a 1 bit, and a pulse distance of 200 μs represents a 0 bit. This distance was chosen to provide sufficient time for the controller to process the last bit and

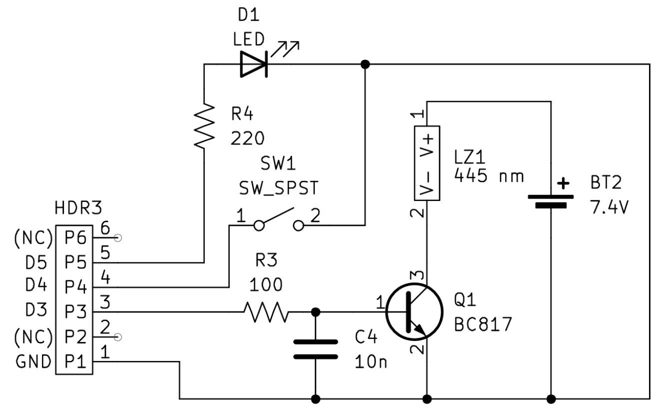

Fig. 1: Schematic for the Transmitter Circuit, showing the 445-450nm laser LZ1 and the Lithium-ion 9V-sized battery for powering it. The switch was a normally-open push button, used to begin the transmission. The low-pass filter combination of R3 and C4 was implemented to allow PWM control of the Q1 BJT transistor. LED D1 was an indicator LED that was not used for data transmission. The header, denoted HDR3, indicates jumper wire connections that attach to the Arduino UNO at the pins specified. (NC) indicates pins that are not connected.

execute read-write operations from memory if necessary, as well as to improve signal integrity by including a substantial separation between pulses. 32-bit long random strings were transmitted using Little-Endian bit order, and a 5 ms delay between strings was used to allow for the received string to be transmitted to a personal computer over a 9600-baud rate UART serial connection to monitor the received bits. All processing was done on-board the 16 MHz-clocked Arduino UNO, with the PC serial connection used only for data validation.

A 1 mW, 445-450 nm off-the-shelf laser module was used as the transmission device for this experiment. Fig. 1 shows the circuit schematic for modulating the laser module. A 9V-sized Lithium-ion battery, with a nominal open-circuit voltage of 7.4 V, was connected to the laser module positive lead, and the negative lead was connected to the collector of an Onsemi BC817-25LT1G NPN BJT transistor to serve as the modulator. The base of the transistor was connected to an RC low-pass filter combination to smooth the driving pulse-width modulated (PWM) output signal from the Arduino digital output pin. This PWM signal operated using a period of 4 μs, and a laser pulse consisted of changing from a 50% duty cycle to a 75% duty cycle for 100 μs. It was found that modulating between these duty cycles, when coupled with the RC low-pass filter, effectively maintained a bias current that maintained the laser channel throughout the entire transmission, and didn't saturate the active filter during a pulse. These duty cycle values were maintained through all experiments.

B. Receiver Circuitry Design

Using a solar panel as a receiver presents some electrical constraints. One consideration is the presence of a DC component from ambient light, which will vary with factors such as depth, water turbidity, water composition, weather, and other

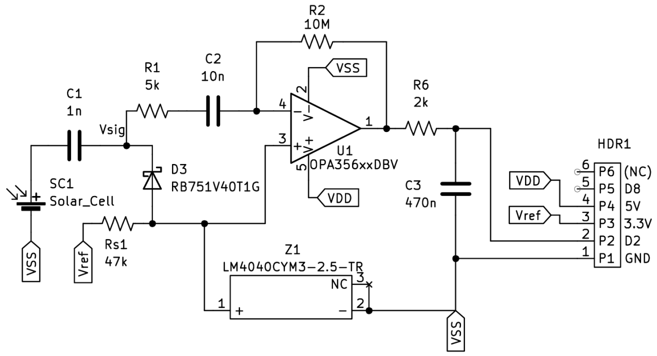

Fig. 2: Schematic for the Receiver Circuit, showing the Solar Panel SC1 and the high-pass op-amp filter. The voltage reference Z1 was used along with a Schottkey diode for the clamping circuit. The header, denoted HDR1, indicates jumper wire connections that attach to the Arduino UNO at the pins specified. (NC) indicates pins that are not connected.

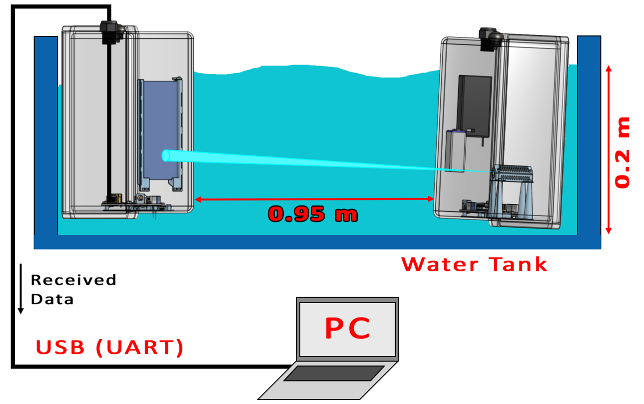

Fig. 3: Experimental setup in a laboratory environment. A 1-yard × 1-yard plastic pool was filled with approximately 0.2 m of clear tap water, sufficient to fully submerge the solar panel and laser, with several centimeters of clearance from the surface to minimize boundary effects. Two containers were placed in the water with a separation of approximately 0.95 m between their nearest faces. The laser was manually aligned to direct the beam onto the center of the solar panel. Received and demodulated messages were transmitted via UART over a USB cable from the receiver Arduino UNO to a personal computer (PC) for data acquisition and validation.

factors. This DC component provides energy that can be used to extend the battery life of the robot, but must be rejected for the communication signal to be received accurately. The solar panel itself consists of a large array of solar cells with considerable capacitance, resulting in a low-pass filter response from the solar panel itself. These factors indicate a bandpass filter be used on the received signal, capable of producing a processed signal composed of short, quick pulses while rejecting very high-frequency noise.

The circuitry for the receiver is shown in Fig. 2. The received signal from the solar array was coupled to a clamping circuit consisting of an Onsemi RB751V40T1G Schottkey diode, a 1 nF ceramic capacitor, and a Microchip Technology LM4040CYM3-2.5-TR shunt voltage reference. An active high-pass filter and inverting amplifier with a $R2/R1$ gain of -2000 was implemented using a Texas Instruments OPA356AIDBVR operational amplifier. The output of this amplifier was then fed to an RC low-pass filter consisting of a 2kΩ resistor and a 470 nF capacitor for noise reduction. This passive filter was a later addition that was implemented via a solderless breadboard, while the rest of the circuit was on a PCB with wires running out from a header to the Arduino. The filtered signal was then connected to a digital input pin (D2) on the Arduino UNO, and a falling-edge interrupt programmed to detect the time between adjacent pulses.

III. Experimental Setup

A. Lab Experiments

An air-channel test with approximately 0.5 m spacing between the transmitter laser and solar panel was conducted under typical commercial LED lighting. Pseudorandom 32-bit numbers were generated by the Arduino "random()" function, with a maximum allowed value of $(7FFFFFFF)_{16}$, since the random() function uses a signed 32-bit integer, and a random number generator seed of 42. The first 10,000 numbers of this sequence were recorded from a serial connection with the transmitter Arduino UNO and saved to serve as evaluation data for future tests. This transmission was also timed via the microcontroller, with 10,000 32-bit long messages requiring 152 seconds to send, producing a maximum data rate of 2.1 kbps. For each subsequent experiment, the receiver sent its received strings from this sequence to the PC to be saved for validation and analysis.

After confirming SHARCS could transmit effectively over the 0.5 m air channel, a 1 yd x 1 yd plastic pool was filled to a depth of about 0.2 m of clear tap water, as shown in the diagram in Fig. 3. The transmitter and receiver hardware were placed in clear plastic containers, which were sealed with silicone aquarium sealant and positioned so that the laser and solar panel pointed out of a clear surface of the container without any embossed text or figures, as shown in Fig. 4. The containers were placed such that the solar panel and laser were approximately 95 cm apart, both fully submerged under the surface to help reduce boundary effects, and angled so that the laser beam was incident near the center of the solar panel. Transmission was triggered by a button press on the transmitter box, with each received 32-bit string recorded and sent over the UART serial connection to be evaluated against the known sequence. Twin experiments were performed underwater under typical commercial LED lighting, which possessed a "cooler" color profile than the in-air test. Then, two additional tests were conducted with the same setup, but with the lights off.

B. Experiments in the Keweenaw Waterway

To assess system performance in realistic freshwater conditions, submerged tests were conducted in the Keweenaw Waterway near Michigan Technological University campus in Houghton, Michigan. The test setup, shown in Fig. 5, mirrors the setup of the laboratory tests.

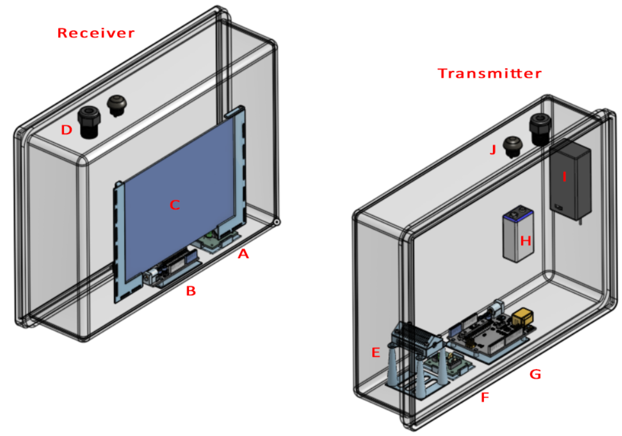

Fig. 4: Models for the Transmitter and Receiver boxes, shown here at scale separated at a distance of 250 mm and configured as they would be for an experiment. The receiver box additionally included a solderless breadboard for the RC lowpass filter, which is not shown here. [A] PCB with receiver circuit. [B] Receiver Arduino UNO. [C] Receiver solar array. [D] Gland for USB cable exit (the adjacent button and mounting hole was not included on the receiver box used in the experiments). [E] Laser module. [F] PCB with transmitter circuit. [G] Transmitter Arduino UNO. [H] Laser power battery. [I] Arduino power battery. [J] Pushbutton to begin the transmission (the adjacent gland and mounting hole was not included on the transmitter box for the experiments). The laser and solar panel are positioned inside the box to face a clear section. The laser is aligned manually at the start of each experiment.

Fig. 5: Experimental setup for daytime testing in the Keweenaw Waterway, replicating the laboratory configuration. Both solar panel and laser were submerged, and the laser was manually aligned to illuminate the center of the solar panel receiver at a distance of 1 m. The receiver enclosure received power via connection to a PC using a USB serial interface, while the transmitter operated independently on battery power.

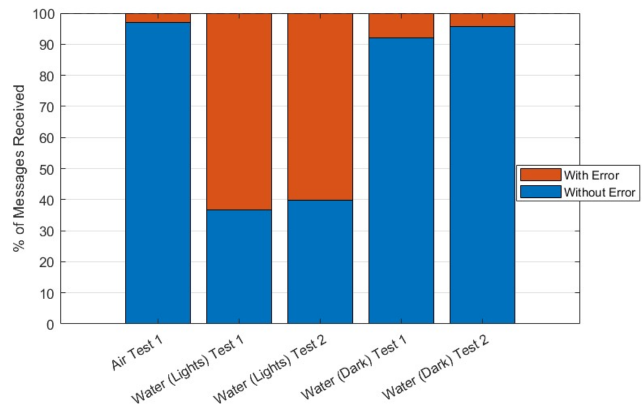

Fig. 6: Transmission accuracy (%) of laser-based communication using a solar panel receiver under five laboratory experiments: one conducted in air, two conducted in water with ambient light on and two with ambient light off. The blue section of the bar indicates the percentage of 32-bit strings received without error, and the red indicates those received with at least 1-bit error.

IV. Results and Discussion

The received messages were compared to the nominal transmitted messages for each test, with each 32 bit string evaluated as a single "message". If the messages matched exactly, it was counted as a message received without error, else it was considered to be received with error, with a breakdown for each test presented in Fig. 6. Additionally, the received and nominal numerical values were converted to binary strings to qualitatively help assess the nature of common errors.

The air channel, 0.5 m test received exactly 10,000 messages, with 97.09% of the messages received without any errors. The most common error for this test was the inclusion of an extra bit in the received message, with 283 of the 291 string errors consisting of one additional received bit. This was also the most common transmission error during the second underwater test with the lights on (39.9% messages transmitted without error), consisting of 4018 of 6010 string errors, and for the two underwater tests in the dark, making up 717 of 792 string errors for the first test (92.08% of messages transmitted without error) and 101 of 105 string errors for the second test (95.8% of messages transmitted without error). The first underwater test began with the laser misaligned, resulting in "Timeout" errors where only some of the peaks were detected. This type of transmission error resulted in 726 additional messages being detected. For the second test, 1826 out of 6787 of the total string errors were the result of an additional bit insertion, and the total success rate, including the timeout errors, was 36.72%. Including the additional messages from link misalignment as errors, a total message success rate for the two tests under the ambient lighting was 38.26%. The overall success rate for the two tests in the dark lab environment was 92.82%.

Other methods, particularly those using QAM-OFDM feature bit error rates ranging from approximately 10^{-2} to 10^{-4}, and Mbps speeds [14], [15], [17], [23]. Due to the use of PDM combined with onboard demodulation on the microcontroller, occasional bit errors and false pulses resulted in message desynchronization. This complicates a comparison between our message error rates and corresponding bit error rates. Our maximum speed of 2.1 kbps was primarily limited by the use of microcontroller hardware that was demodulating while receiving, reflecting an applied scenario, rather than demodulating offline. Pulse distances were limited by the speed of the required read-write operations, and the 5 ms delay between messages may be shorter in a controls scenario where sending out the received messages via serial connection is not required.

Ambient light was found to have significant effects on error rates when transmitting through water, with brighter ambient lighting significantly reducing the efficacy of the transmission both in the lab environment and in the Keweenaw Waterway. Testing in the Keweenaw Waterway revealed that sunlight was strong enough to prevent any signal from being received at all, though the laser point could be seen incident on the outside of the receiver box. Solar array saturation and greater noise, which would be amplified by the high-pass filter on the receiver PCB, are most likely the phenomena primarily responsible for this decreased performance. These effects may be reduced with more selective design of a band-pass filter, rather than a high-pass filter with a subsequent passive RC lowpass filter, along with a blue light filter in front of the solar array.

V. Conclusion

This paper introduces SHARCS, a novel underwater optical communication system for cost-effective, small underwater AUVs running on embedded system hardware and with a solar array receiver. It presents a pulse distance modulation scheme and accompanying circuitry for the transmission and decoding of data via a commercially-available blue-light laser module. Experiments with Arduino UNO hardware reveal that SHARCS is successful for short-range communication.

In future work, measures to reduce the ambient light effects should be considered. A finely-tuned active bandpass filter can also be considered to improve the performance of the system. Considering these improvements, SHARCS shows promise for wireless optical underwater control, and would help open the door to small, low-power, low-cost AUVs.

Acknowledgment

This work was supported in part by May Waters and Sharmilee Nowshin. The authors would like to thank them for their assistance with experimental data collection and assembly of the prototype. Further, the first author would like to thank Douglas Powers for creative inspiration.

References

[1] R. Bogue, "Underwater robots: a review of technologies and applications," *The Industrial Robot*, 2015.

[2] S. Chutia, N. M. Kakoty, and D. Deka, "A review of underwater robotics, navigation, sensing techniques and applications," *Association for Computing Machinery*, 2017.

[3] J. Yuh, G. Marini, and D. R. Blidberg, "Applications of marine robotic vehicles," *Intelligent Service Robotics*, 2011.

[4] A. Veerle, K. R. Huvenne, L. Marsh, C. Lo Iacono, T. Le Bas, and R. B. Wynn, *Submarine Geomorphology*. Springer Geology, 2017, ch. ROVs and AUVs, pp. 93–108.

[5] F. A. Azis, M. S. M. Aras, M. Rashid, M. N. Othman, and S. Abdullah, "Problem identification for underwater remotely operated vehicle (rov): A case study," in *International Symposium on Robotics and Intelligent Sensors 2012 (IRIS 2012)*. Procedia Engineering, 2012, pp. 554–560.

[6] M. S. Ziegler and J. E. Trancik, "Re-examining rates of lithium-ion battery technology improvement and cost decline," *Energy Environmental Science*, vol. 14, 2021.

[7] N. Oceanic and A. Administration. (2025). [Online]. Available: https://web.archive.org/web/20250405115813

[8] Y. Lou and N. Ahmed, *Underwater Communications and Networks*, ser. Textbooks in Telecommunication Engineering. Springer, 2021, ch. Signal Processing in UWAC, pp. 57–83.

[9] F. Campagnaro, F. Steinmetz, and B.-C. Renner, "Survey on low-cost underwater sensor networks: From niche applications to everyday use," *Journal of Marine Science and Engineering*, 2023.

[10] Z. Zeng, S. Fu, H. Zhang, Y. Dong, and J. Cheng, "A survey of underwater optical wireless communications," *IEEE Communications Surveys Tutorials*, 2017.

[11] J. Xu and Y. Zhang, "Underwater wireless optical communications: From the lab tank to the real sea," *Journal of Lightwave Technology*, 2022.

[12] C. Chang, X. Han, G. Li, P. Li, W. Nie, P. Liao, C. Li, W. Wang, and X. Xie, "Extending uwoc system applications through photon transmission dynamics study in harbor waters," *Applied Sciences*, 2024.

[13] X. Yang, Z. Tong, Y. Dai, X. Chen, H. Zhang, H. Zou, and J. Xu, "100 m full-duplex underwater wireless optical communication based on blue and green lasers and high sensitivity detectors," *Optics Communications*, 2021.

[14] J. Xu, D. Lin, X. Yu, Y. Song, M. Kong, F. Qu, J. Han, W. Jia, and N. Deng, "Underwater laser communication using and ofdm-modulated 520-nm laser diode," *IEEE Photonics Technology Letters*, 2016.

[15] H. M. Oubei, J. R. Duran, B. Janjua, H.-Y. Wang, C.-T. Tsai, Y.-C. Chi, T. K. Ng, H.-C. Kuo, J.-H. He, L.-G.-R. Alouini, Mohamed-Slim, and B. S. Ooi, "4.8 gbit/s 16-qam-ofdm transmission based on compact 450-nm laser for underwater wireless optical communication," *Optics Express*, 2015.

[16] D. Chen, Z. Li, J. Wang, H. Lu, R. Hao, K. Fan, J. Jin, Q. Wang, and S. Wu, "Experimental study of laser spot tracking for underwater optical wireless communication," *Optics Express*, 2024.

[17] M. Kong, B. Sun, R. Sarwar, J. Shen, Y. Chen, F. Qu, J. Han, J. Chen, H. Qin, and J. Xu, "Underwater wireless optical communication using a lens-free solar panel receiver," *Optics Communications*, 2018.

[18] Z. Tong, X. Yang, H. Zhang, Y. Dai, X. Chen, and J. Xu, "Series-connected solar array for high-speed underwater wireless optical links," *Optics Letters*, 2022.

[19] Z. Tong, X. Yang, Y. Gao, H. Zhang, Y. Zhang, X. Wang, and J. Xu, "A long-distance underwater wireless optical link enabled by a solar array with a baseline compensator," *IEEE Photonics Journal*, 2023.

[20] F. Dang, S. Nasreen, and F. Zhang, "Dmd-based background flow sensing for auvs in flow pattern changing environments," *IEEE Robotics and Automation Letters*, vol. 6, no. 3, pp. 5207–5214, 2021.

[21] F. Dang and F. Zhang, "Distributed flow estimation for autonomous underwater robots using proper orthogonal decomposition-based model reduction," *Journal of Dynamic Systems, Measurement, and Control*, vol. 141, no. 7, p. 071010, 2019.

[22] F. Dang and F. Zhang, "Distributed flow estimation for autonomous underwater robots using pod-based model reduction," in *2018 IEEE Conference on Decision and Control (CDC)*. IEEE, 2018, pp. 4453–4458.

[23] M. Zhang, Y. Chen, and M. Li, "Vision-aided localization for ground robots," in *2019 IEEE/RSJ International Conference on Intelligent Robots and Systems (IROS)*. IEEE, 2019, pp. 2455–2461.